

NUMERICAL SIMULATION OF THE THERMO-HYDRAULIC PERFORMANCE OF FAN SUPPLIED FIN-TUBE HEAT EXCHANGERS

Maicon Waltrich, maicon@polo.ufsc.br

Christian J. L. Hermes, hermes@polo.ufsc.br

Cláudio Melo, melo@polo.ufsc.br

POLO National Institute of Science and Technology of Refrigeration and Thermophysics, Federal University of Santa Catarina
88040-970, Florianópolis, SC, Brazil, Phone: ++55 48 3234 5691

Joaquim M. Gonçalves, joaquim@sj.cefetsc.edu.br

IF-SC, 88103-310, Rua José Lino Kretzer 608, São José, SC, Brazil, Phone: ++55 48 3381 2800

Abstract: *The present paper puts forward a first-principles numerical model to simulate the thermo-hydraulic performance of fan supplied compact fin-tube heat exchangers for light commercial refrigeration applications, i.e., heat duties ranging from 0.5 to 2.0 kW. The model is based on the mass, momentum and energy conservation equations applied to both the refrigerant and the air streams. The model predictions have been validated against experimental data obtained in-house and elsewhere. It has been found that the proposed model reproduces the air side heat transfer and pressure drop data within $\pm 10\%$ and $\pm 15\%$ error bands, respectively. Moreover, the model was used to assess the thermal-hydraulic performance of a gas cooler running with supercritical CO_2 as working fluid. Although the model was developed and validated for condensers and gas coolers, it can be easily used to assess the thermo-hydrodynamic performance of dry-coil fin-tube evaporators.*

Keywords: *tube-fin, condenser, gas cooler, fan-coil, modeling, simulation*

1. INTRODUCTION

The energy consumed by refrigeration and air conditioning appliances in Brazil approaches 50,000 GWh per year when both the commercial and household sectors are accounted for. Such a figure is practically 50% of the energy produced annually by the Itaipu hydropower plant (ANEEL, 2003). This fact not only highlights the need for an energy utilization rationale but also points out the urgency of more efficient refrigeration systems. It is well-known that part of the energy consumption is due to the irreversible thermodynamic processes that take place in each of the system components, among which the heat exchangers present the lower cost / benefit ratio.

Most of the heat exchangers used in small-size refrigeration and air conditioning appliances are of the fin-tube type, in which the air flows externally over extended surfaces whereas the refrigerant flows inside the coil. Performance analysis of this kind of heat exchanger is usually carried out through experimental tests. A faster and less costly alternative consists of using mathematical models to simulate the thermo-hydraulic behavior of the heat exchanger coils. The simulation not only rationalizes the number of prototypes and experiments needed but also permits the heat exchanger optimization based on both component-level (e.g., j , f) and system-level (e.g., COP) performance indicators.

Nonetheless, the major part of the simulation tools available for heat exchanger performance assessment (e.g., Domanski, 1991, Judge *et al.*, 1997; Bensafi *et al.*, 1997; Corberán and Melón, 1998, Liang *et al.*, 2001, Jiang *et al.* 2006, Garcia *et al.*, 2007a, b, Ge and Cropper, 2008) does not account for the hydrodynamic interaction between the heat exchanger pressure drop and the fan characteristics. Recent studies (Weber, 2007; Waltrich, 2008; Waltrich, 2009) suggest that the fan-coil interaction plays an important role on either performance or cost-driven design processes since any geometric modification also changes, as a side-effect, the hydrodynamic point of operation of the fan-coil system.

Therefore, a mathematical model to simulate the thermo-hydraulic performance of fin-tube heat exchanger, which accounts for the fan-coil hydrodynamic interaction, is proposed herein. The model results were compared with experimental data obtained using a wind-tunnel test facility specially designed for assessing the performance of condenser coils of light commercial refrigerators, with heat duties ranging from 0.5 to 2.0 kW. The model predictions for the heat transfer rate and pressure drop agreed with the experimental data within 10 and 15% error bands, respectively. Moreover, the model reproduced quite well the experimental trends in terms of temperature profiles.

2. MATHEMATICAL FORMULATION

The development of mathematical models for numerical analysis of fin-tube heat exchangers relies on the solution of air, refrigerant and heat flows over the fins and tubes. These phenomena are governed by the mass, momentum and energy conservation equations, whose solution is complex and demands an enormous computational effort. In order to balance model accuracy and mathematical complexity, the heat exchanger model proposed herein was divided into two lumped sub-models, named thermal and hydrodynamic. The former provides the heat transfer rate and the thermodynamic states of both air and refrigerant streams at the outlet ports, whereas the latter calculates the air flow rate supplied by the fan at the point of operation. Both sub-models are described in detail in the following sections.

2.1. Thermal sub-model

The thermal sub-model was divided into two domains, named air and refrigerant sides. The thermal resistances due to thermal conduction in the tube and fin walls were neglected as $Biot \sim 10^{-3}$. Both air and refrigerant flows are modeled as one-dimensional, steady-state, purely advective flows as $Peclet \sim 10^3$. Therefore, the air and refrigerant flows were modeled based on the following energy balances applied to the control volume illustrated in Fig. 1:

$$m_r(h_{i,r} - h_{o,r}) + Q_{cv} = 0 \quad (1)$$

$$m_{a,cv}c_{p,a}(t_{i,a} - t_{o,a}) - Q_{cv} = 0 \quad (2)$$

where m_r and $m_{a,cv}$ are the refrigerant and air mass flow rates through the control volume [kg/s], respectively, h is the specific enthalpy of the refrigerant [J/kg], and the indices i and o refer to the inlet and outlet ports of the control volume, respectively. The heat transfer rate Q_{cv} was calculated based on the heat exchanger effectiveness, as follows:

$$Q_{cv} = \pm \varepsilon C_{min}(t_{i,h} - t_{i,c}) \quad (3)$$

where “ \pm ” should read “ $-$ ” when the refrigerant releases heat to the air stream (condensers and gas coolers) and “ $+$ ” when the refrigerant receives heat from the air stream (evaporators). In addition, $C_{min} = \min(m_r c_{p,r}, m_{a,cv} c_{p,a})$ is the lowest thermal capacity [W/K] of the streams, and $t_{i,h}$ and $t_{i,c}$ are the temperatures of the hot and cold streams at the entrance ports [K], respectively. The control volume effectiveness ε was calculated from the following equation for mixed, cross-flow, single-pass heat exchanger (Kays and London, 1984):

$$\varepsilon = 1 - \exp(NTU^{0.2} C_r^{-1} (\exp(-C_r NUT^{0.78}) - 1)) \quad (4)$$

where $C_r = C_{min}/C_{max}$, $NTU = UA/C_{min}$ is the number of transfer units. The thermal conductance UA was obtained from,

$$UA^{-1} = (\alpha_r A_r)^{-1} + (\alpha_a (A_t + \eta_f A_f))^{-1} \quad (5)$$

where η_f is the fin efficiency calculated through the procedure introduced by Schmidt (1945).

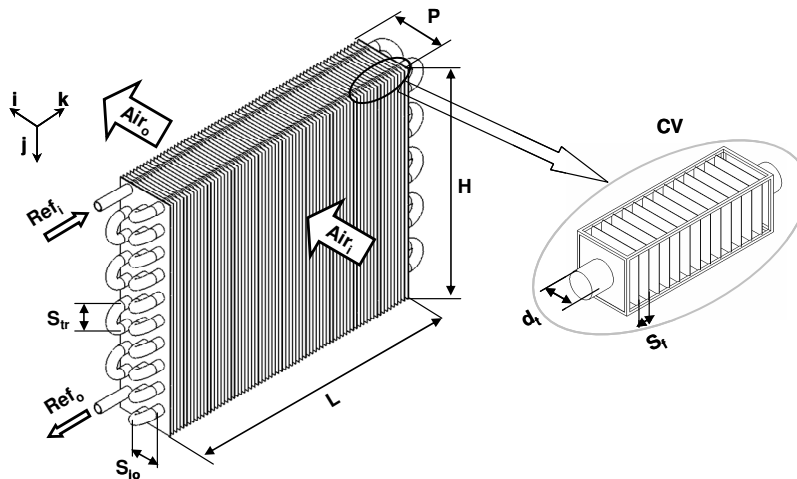


Figure 1. Schematic representation of the heat exchanger discretization.

Equations (1) to (5) were solved following the refrigerant coil arrangement (see Fig. 1) assuming that each control volume behaves as an individual heat exchanger. Therefore, although the air and refrigerant streams were modeled as one-dimensional, the overall simulation model takes into account the multidimensional effect of the coil circuitry.

The heat transfer coefficients required by the model were obtained from empirical correlations. The air-side heat transfer coefficients were selected based on an experimental study performed using a wind-tunnel facility designed for this purpose, whereas the refrigerant-side heat transfer coefficients were obtained by Gnielinski's (1976) correlation for single-phase flows and Bassi and Bansal's (2003) correlation for convective condensation of refrigerant HFC-134a. The thermophysical properties of air and refrigerant were calculated using the REFPROP7 software (Lemmon *et al.*, 2002) linked to the EES platform (Klein, 2004).

2.2. Hydrodynamic sub-model

The hydrodynamic sub-model involves not only the heat exchanger pressure drop calculation, but also the air flow rate supplied by the fan at the point of operation, as shown in Fig. 2. The pressure drop over the heat exchanger was calculated as follows (Kays and London, 1984):

$$\Delta p = \frac{m_a^2}{2\rho_{i,a}A_{min}^2} \left[\left(1 - \left(\frac{A_{min}}{A_{face}} \right)^2 \right) \left(\frac{\rho_{i,a}}{\rho_{o,a}} - 1 \right) + 2f \frac{A_t + A_f}{A_{min}} \frac{\rho_{i,a}}{\rho_{i,a} + \rho_{o,a}} \right] \quad (6)$$

where $\rho_{i,a}$ and $\rho_{o,a}$ are the air densities at the inlet and outlet ports, f is the Darcy friction factor, and A_{min} is the minimum air flow passage area [m²].

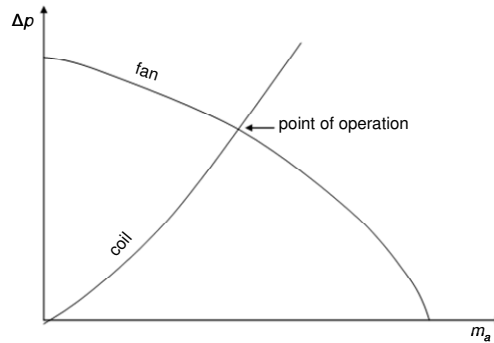


Figure 2. Schematic representation of the fan-coil hydrodynamic interaction.

As shown in Fig. 2, the point of operation is defined by the intersection between the heat exchanger pressure drop, given by Eq. (6), and the fan performance curve, represented here by the following polynomial fit of 6th degree:

$$\Delta p = \sum_{i=0}^6 a_i m_a^i \quad (7)$$

Furthermore, the fan pumping power is given by:

$$W_v = \frac{\Delta p}{\eta_v} \frac{2m_a}{\rho_{i,a} + \rho_{o,a}} \quad (8)$$

where η_v is the overall fan efficiency, also represented by a 6th degree polynomial fit:

$$\eta_v = \sum_{i=0}^6 b_i m_a^i \quad (9)$$

2.3. Numerical Scheme

Each tube is divided into non-overlapping control volumes, all of them with the same length. The control volume position is defined by coordinates i, j and k , as shown in Fig. 3. The coil discretization begins at the refrigerant inlet port ($i=1, j=1, k=1$) and follows the coil circuit until the refrigerant outlet port ($i=1, j=1, k=kk$). The refrigerant flow direction in each tube is defined by vector $\mathbf{S}[n]$, where n is the tube index. In case where the flow is entering the paper sheet (see Fig. 3), $\mathbf{S}[n] = +1$, otherwise $\mathbf{S}[n] = -1$. The refrigerant circuitry must be informed by the user in matrix $\mathbf{OT}[i, j]$, whose elements indicate to the spatial location of the tube in the heat exchanger coil, as illustrated in Fig. 3. It is worthy noting that in the first tube ($\mathbf{OT} [1,1]$), the refrigerant enters the paper sheet, while it leaves the sheet in the second tube ($\mathbf{OT} [2,1]$).

For each control volume, there are input variables that ought to be informed, such as air temperature and refrigerant enthalpy, and output variables that are obtained through the solution of the governing equations and then used as input data for the next control volume. The air flow through each control volume $m_{a,cv}$ is calculated dividing the overall air flow rate m_a by the number of control volumes on the transversal direction to the flow. The overall heat transfer rate is obtained by summing the local heat transfer rates calculated for each control volume.

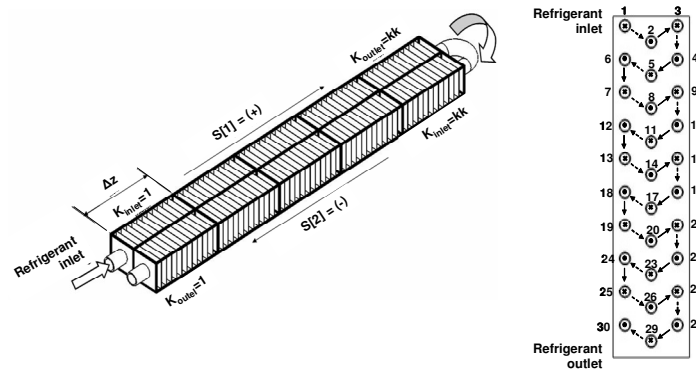


Figure 3. Schematic representation of the refrigerant circuitry.

The solution algorithm is based on two loops, as shown in Fig. 4. First, an iterative process solves equations (6) and (7) to obtain the air flow rate supplied by the fan at the point of operation. Then, equations (1) to (5) are solved for each control volume through a one-way march following to the refrigerant circuit. The march is performed in two steps. First, the refrigerant flow is solved using estimated air temperatures, which are then corrected by Eq. (2). The procedure is repeated until convergence is achieved, i.e., when the largest temperature difference between two successive iterations is less than 0.1°C.

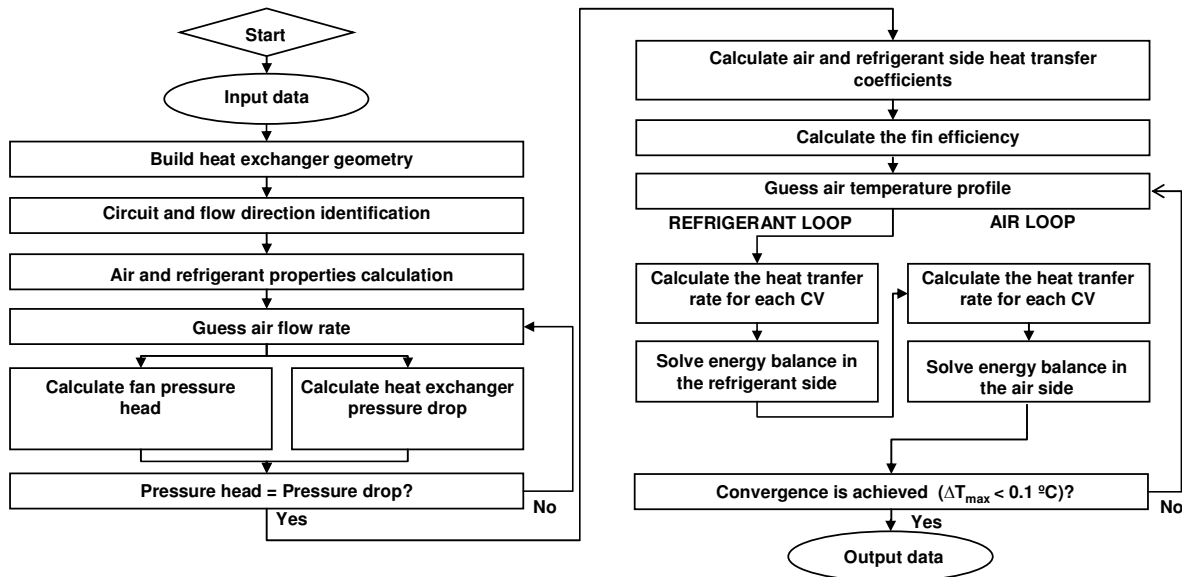


Figure 4. Solution algorithm.

3. EXPERIMENTAL WORK

3.1. Experimental Apparatus

Experiments were carried out with a series of fin-tube heat exchanger samples particularly designed for light commercial refrigeration applications. The tests were performed using a wind-tunnel calorimeter facility (see Fig. 5) specially constructed by Weber (2007) for testing tube-fin heat exchangers according to the ANSI/ASHRAE 33 (2000) standard. The wind-tunnel comprises the following components: a 0.55 x 0.55 m² test section; a set of electrical heaters and a refrigeration system for controlling the air temperature at the test section entrance; a variable-speed radial fan for controlling the air flow rate. The wind-tunnel walls consist of two 1 mm thick galvanized steel sheets that embrace a 400 mm thick glass wool insulating layer. Additional 32 mm thick rubber insulation was applied on both internal and external sides of the test section. The ductwork was built modularly to facilitate both assembly and disassembly operations. Windows were also placed along the tunnel to provide quick access to the test section. The joints of the windows and flanges were sealed with silicone rubber to avoid air leakage.

The following measurement instruments were also employed: two differential pressure transducers for measuring the coil and nozzle pressure drops with an uncertainty of $\pm 0.5\%$; two grids of nine T-type thermocouples placed before and after the heat exchanger with measurement uncertainties of $\pm 0.2^\circ\text{C}$; immersion T-type thermocouple probes for measuring the refrigerant temperatures at the entrance and exit ports with an uncertainty of $\pm 0.2^\circ\text{C}$; T-type thermocouples fixed on each heat exchanger return bend for measuring the temperature profile along the coil with an uncertainty of $\pm 0.2^\circ\text{C}$; a convergent nozzle for measuring the air flow rate according to the ANSI/ASHRAE 41.2 (1987) standard. The experimental apparatus operates with air flow rates ranging from 170 and 2000 m^3/h , refrigerant mass flow rates up to 250 kg/h , and refrigerant pressures up to 20 bar.

The refrigerant circuit, illustrated in Fig. 6, emulates the working conditions typically observed in a condenser of light commercial refrigeration appliances. From point 1 to point 2, the liquid refrigerant evaporates inasmuch receives heat from a hot-water thermostatic bath. The degree of superheating is controlled by heaters (process 2-3) placed before the test section, where the refrigerant is re-condensed (process 3-4). The refrigerant is then subcooled by a cold-water thermostatic bath (process 4-5), and liquid refrigerant is then pumped back to the hot-water heat exchanger, closing the circuit. Although the facility was initially designed to work with HFC-134a as working fluid (Weber, 2007), the apparatus was adapted to operate with water as well. The original refrigerant circuit was replaced by a secondary water circuit, where tap water is pumped through the heat exchanger coil. The water temperature at the heat exchanger inlet is controlled by 800 W electrical heaters.

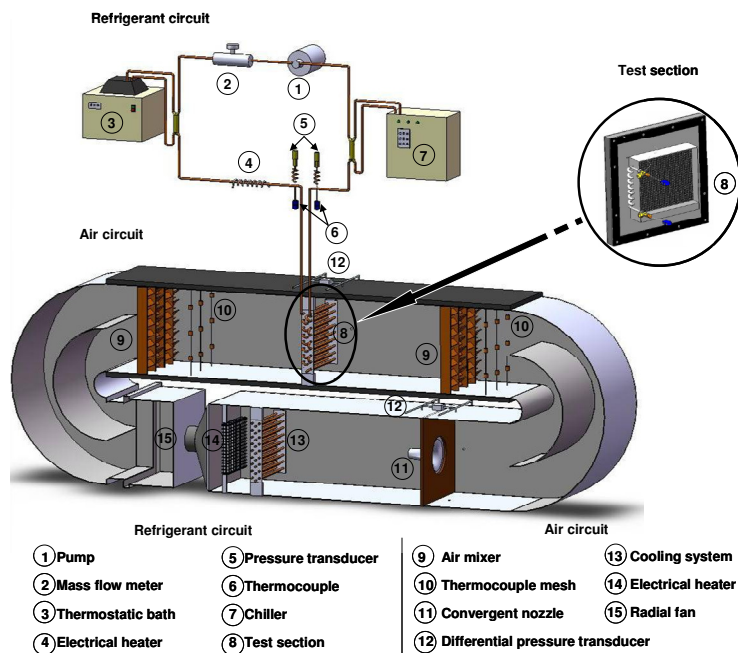


Figure 5. Schematic representation of the wind-tunnel facility.

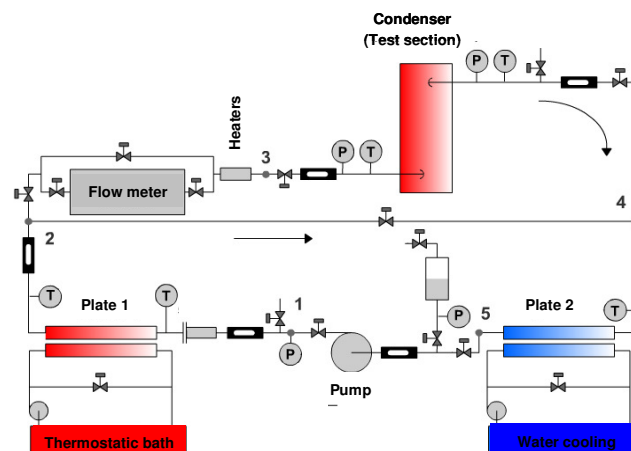


Figure 6. Schematic representation of the refrigerant circuit (Weber, 2007).

3.2. Test Planning

In total, 12 fin-tube heat exchangers samples were tested, whose geometries are indicated in Tab. 1. The geometries were selected so that the flow passage areas correspond to those commonly observed in condensers. The tests were conducted at various operating conditions, totalizing 54 experimental runs. First, a single heat exchanger (# 1) was tested using water as working fluid. Tests were performed varying the water temperature for a fixed flow rate (10 kg/h) and also varying the flow rate for a fixed inlet temperature (50°C). Later, all samples were tested using HFC-134a as working fluid. The heat transfer rate and the pressure drop were measured under typical operating conditions of light commercial refrigeration appliances: the condensing temperature was controlled at 40°C, the superheating and subcooling degrees were fixed at 10°C and 5°C, respectively, and the air flow rate was ranged from 250 to 1400m³/h. The test results were used for both correlation selection and model validation exercises.

Table 1. Geometric characteristics of tested heat exchangers.

Sample	F_f	S_{ir}	S_{io}	N_{lo}	d_t	δ_f	L	H	P	Fin
	[mm]	[mm]	[mm]	[-]	[mm]	[mm]	[mm]	[mm]	[mm]	[-]
1	4.05	25.6	21.67	3	9.5	0.140	304	256	65	flat
2	3.17	25.6	21.67	3	9.5	0.140	304	256	65	flat
3	2.53	25.6	21.67	3	9.5	0.140	304	256	65	flat
4	3.88	25.5	20.33	3	9.5	0.140	380	153	61	flat
5	2.86	25.5	20.33	3	9.5	0.140	380	153	61	flat
6	2.48	25.5	20.33	3	9.5	0.140	380	153	61	flat
7	3.88	25.5	20.33	3	9.5	0.140	380	153	61	louver
8	2.86	25.5	20.33	3	9.5	0.140	380	153	61	louver
9	2.48	25.5	20.33	3	9.5	0.140	380	153	61	louver
10	4.34	25.6	22.50	2	9.5	0.140	304	256	45	flat
11	3.04	25.6	22.50	2	9.5	0.140	304	256	45	flat
12	4.34	25.6	22.50	2	9.5	0.140	304	256	45	flat

4. RESULTS AND DISCUSSION

In order to select the most appropriate air-side pressure drop and heat transfer correlations, the experimental results were compared with the model predictions using various correlations available from the literature (Wang *et al.*, 1996; Abu *et al.*, 1998; Kim *et al.*, 1999; Wang *et al.*, 2000). Figure 7.a compares the measured heat transfer rates with the simulated counterparts, where it can be noted that all the mentioned correlations, but that of Abu *et al.* (1998), provided good results, with differences within $\pm 10\%$ error bands. Figure 7.b compares the measured pressure drops with the simulated counterparts, where it can be observed that the model tends to overestimate the experimental pressure drops in cases when the correlations of Wang *et al.* (1996) and Kim *et al.* (1999) were adopted. The correlations of Abu *et al.* (1998) and Wang *et al.* (2000) showed satisfactory results, with predictions within $\pm 15\%$ error bands. Therefore, the choice of the best correlation was based on the root mean square (RMS) deviation between the measured and simulated data. As can be seen in Tab. 2, the correlation of Wang *et al.* (2000) provided the best matching between simulated and experimental data.

Table 2. Root mean square errors for various heat transfer and pressure drop correlations.

Correlation	Heat transfer	Pressure drop
Wang <i>et al.</i> (1996)	0.058	0.484
Abu <i>et al.</i> (1998)	0.121	0.178
Kim <i>et al.</i> (1999)	0.043	0.638
Wang <i>et al.</i> (2000)	0.050	0.162

Figure 8.a compares a simulated temperature profile with the measured counterpart obtained using HFC-134a as the working fluid. First, it can be noted that the difference between the simulated and measured refrigerant temperatures at the inlet and outlet ports are lower than 0.5°C. In addition, it was observed that temperature differences between the refrigerant and the tube walls as high as 2°C were observed, which can be explained by the thermal resistance of the

refrigerant flow. Moreover, Fig. 8.a shows that the simulated temperature profile reproduces reasonably well the experimental trends, particularly the superheated and subcooled regions. Figure 8.b compares the simulated temperature profiles with the experimental counterparts in cases where water was used as the working fluid. Again, the model reproduced satisfactorily well the experimental trends.

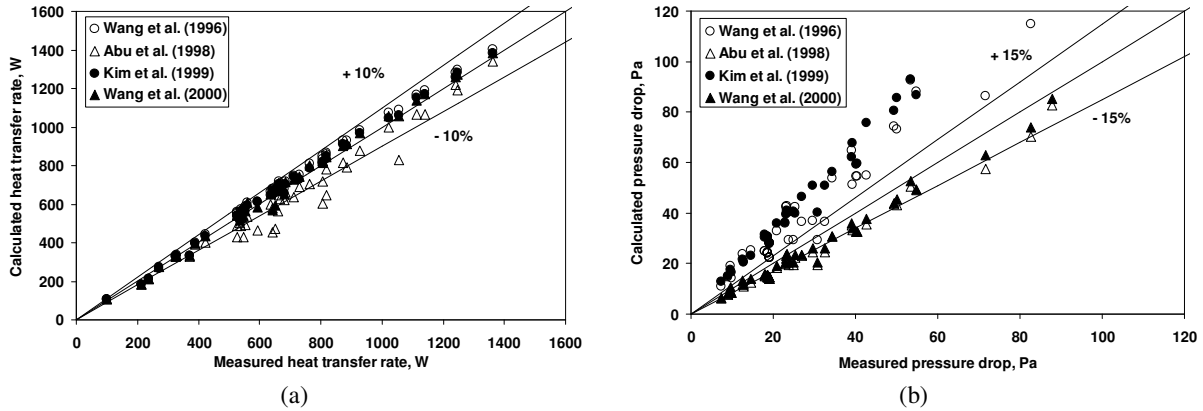


Figure 7. Measured versus simulated results using various heat transfer (a) and pressure drop (b) correlations.

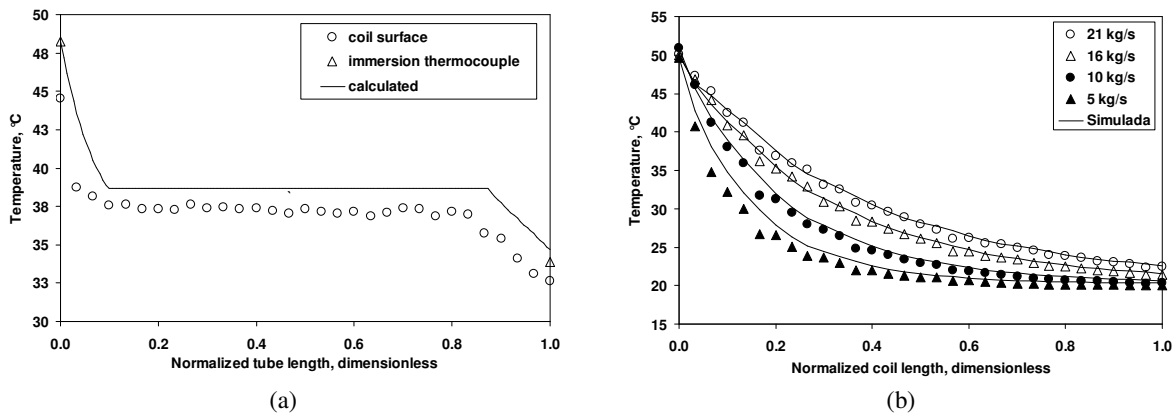


Figure 8. Measured versus simulated temperature profiles for HFC-134a (a) and water (b).

Figure 9 compares the model predictions for the heat transfer rate (Fig. 9.a) and pressure drop (Fig. 9.b) with the experimental counterparts, where it can be seen that model is able to predict 92% of the experimental heat transfer data within a 10% error band, and 88% of the pressure drop data within a 15% error band.

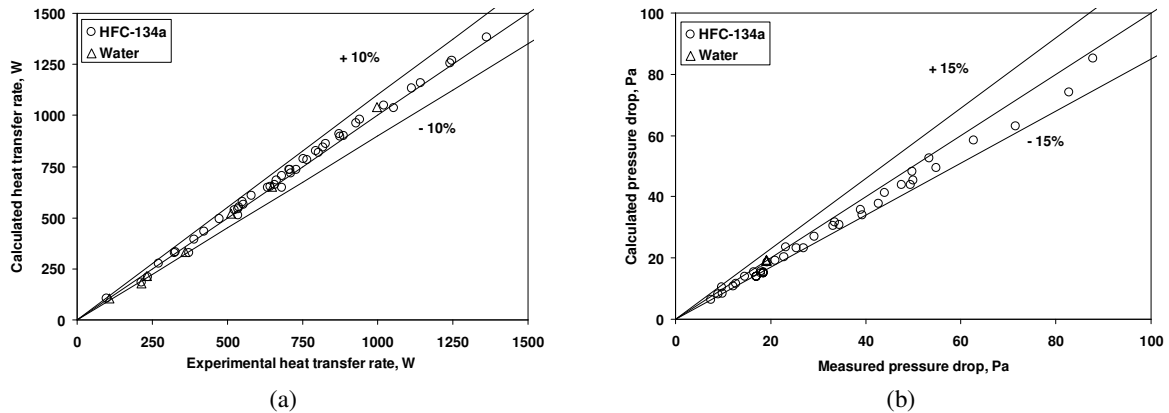


Figure 9. Measured versus simulated heat transfer rate (a) and pressure drop (b) for HFC-134a and water.

Figure 10.a compares the simulated temperature profile with experimental data gathered by Ge and Cropper (2008) using supercritical CO₂ as working fluid. It can be observed that the proposed model reproduces satisfactorily the temperature distribution along the coil, with differences between the calculated approach temperature (i.e., the refrigerant temperature at the gas cooler outlet port) and the measured counterpart below 2°C for 77% of the data points. The model also proved to be able to reproduce satisfactorily the experimental trends. Figure 10.b shows that the model is able to predict the heat transfer rates for more than 86% of the experimental data points of Ge and Cropper (2008) with errors within 10% bands.

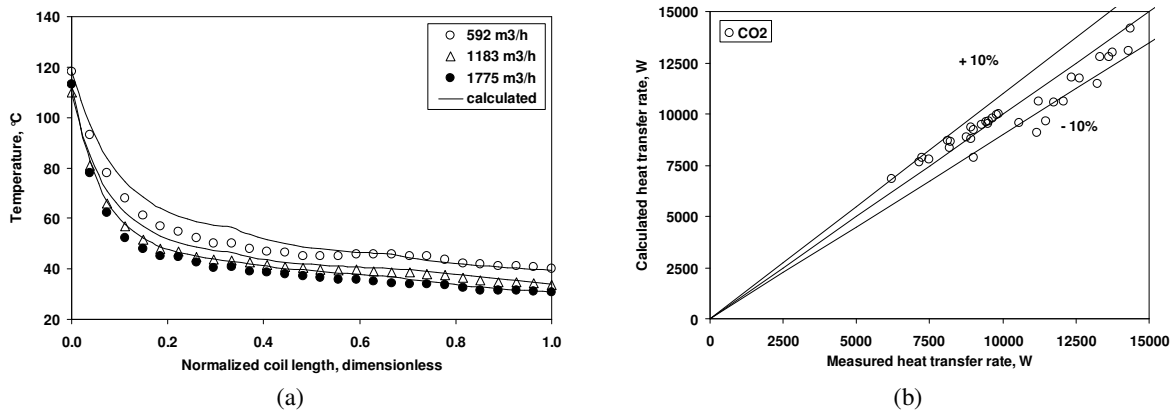


Figure 10. Model predictions versus Ge and Cropper's (2008) data for temperature profiles (a) and heat transfer rate (b).

The model was also used to assess the influence of the fan-coil hydrodynamic interaction on the performance of a gas cooler running with supercritical CO₂ as working fluid. During the simulations, the heat exchanger envelope was kept fixed (length x height x depth = 304 mm x 254 mm x 66 mm), whereas the numbers of tubes and fins were varied. The coefficients of the fan used in the analysis are $a_0=79.2$, $a_1=-124.8$, $a_2=-1007$, $b_0=-0.036$, $b_1=3.0$ and $b_2=-11.4$.

Figure 11 illustrates the influence of the number of tubes and fins on both heat transfer rate (Fig. 11.a) and air flow rate (Fig. 11.b). It was observed that a change from 10 to 8 fins per inch, which decreased the heat transfer surface by 20%, reduced the heat transfer rate by 1% only. This was so as the pressure drop also decreased, increasing the air flow rate supplied by the fan (see Fig. 11.b). Similarly, the reduction from 11 to 10 tubes in the cross section decreased the heat transfer rate by 2% only. Such an analysis was only feasible since the fan and the coil have been analyzed together. If the air flow was held constant, unrealistic predictions of the heat transfer rate could mislead the conclusions.

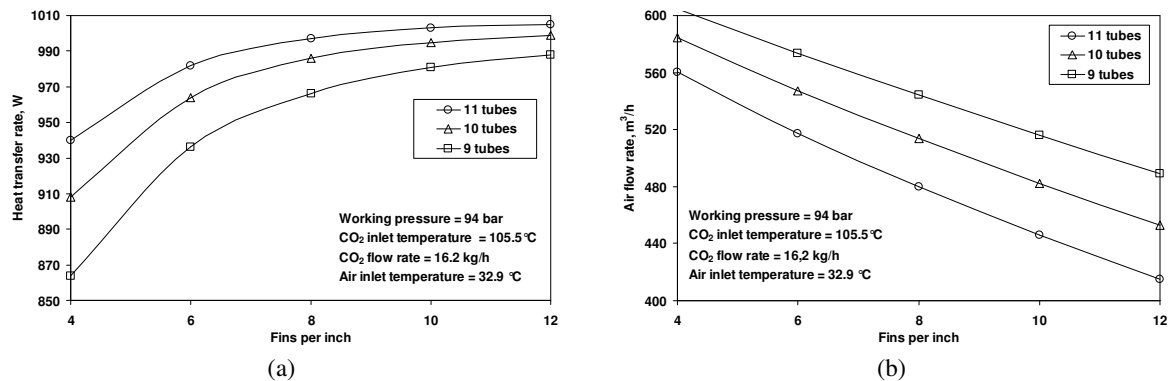


Figure 11. Performance assessment of a fan supplied gas cooler in terms of heat transfer (a) and air flow (b) rates

5. SUMMARY AND CONCLUSIONS

A numerical simulation model for fan supplied compact fin-tube heat exchangers was presented. The model predictions for the temperature profiles, heat transfer rate and the pressure drops were compared with experimental data obtained in-house using a purpose-built experimental apparatus that operates with HFC-134a and water as working fluids. It was observed that the model is able to predict the overall performance of the heat exchanger in terms of heat transfer rate and pressure drop with errors within 10% and 15% bands, respectively. The model predictions of the temperature profiles followed closely the experimental trends. Additional comparisons were carried out using experimental data obtained elsewhere for a gas cooler that operates with supercritical CO₂ as working fluid. It was

observed that the model provides satisfactory results for both the heat transfer rate and pressure drops. Finally, the model was used to analyze the thermo-hydraulic behavior of a fan supplied gas cooler, showing that reductions of 20% in the heat transfer surface decreased the heat transfer rate by 1% only. Although the model was originally developed for condensers and gas coolers, it can be easily extended for evaporators if a heat transfer correlation for the evaporative flow is provided.

6. ACKNOWLEDGMENTS

The authors duly acknowledge the financial support from the Brazilian funding agencies CNPq and FINEP.

7. REFERENCES

- Abu, M. M., Johns, R. A., Heikal, M. R., 1998, "Performance characteristics correlation for round tube and plate finned heat exchangers", *Int. J. of Refrigeration*, 21, 507-517.
- ANEEL, 2005, "Atlas de Energia Elétrica do Brasil", 2º Edição, Brasília, pp 160.
- ASHRAE 33, 2000, "Method of Testing Forced Circulation Air Cooling and Air Heating Coils".
- ASHRAE 41.2, 1987, "Standard Methods for Laboratory Airflow Measurement".
- Bassi, R., Bansal, P.K., 2003, "In-tube condensation of mixture of R134a and ester oil: empirical correlations", *International Journal of Refrigeration*, Vol. 26: pp. 402-409.
- Bensafi, A., Borg, S., Parent, D., 1997, CYRANO: "A computational model for the detailed design of plate-fin-and-tube heat exchangers using pure and mixed refrigerants", *Int. J. Refrigeration*, 20, 218-228.
- Corberan, J.M., Melon, M.G., 1998, "Modeling of plate finned tube evaporators and condensers working with R134a", *International Journal of Refrigeration*, Vol. 21: pp. 273-284.
- Domanski, P. A., 1991, "Simulation of an evaporator with non-uniform one-dimensional air distribution", *ASHRAE Transactions*, Vol. 97: pp. 793-802.
- García, J.R.C., Vera, F.G., Corberán, J.M.S., González, J.M., Fuentes, D.D., 2007a, "Assessment of boiling heat transfer correlations in the modeling of fin and tube heat exchangers", *International Journal of Refrigeration*, Vol. 30: pp. 1004-1017.
- García, J.R.C., Vera, F.G., Corberán, J.M.S., González, J.M., Fuentes, D.D., 2007b, "Assessment of condensation heat transfer correlations in the modeling of fin and tube heat exchangers", *International Journal of Refrigeration*, Vol. 30: pp. 1018-1028.
- Ge Y. T., Cropper R. T., 2008, "Simulation and performance evaluation of finned-tube CO₂ gas coolers for refrigeration systems", doi: 10.1016/j.applthermaleng. 2008.05.013.
- Gnielinski, V., 1976, "New equations for heat and mass transfer in turbulent pipe and channel flow", *International Chemical Engineering*, Vol. 16: pp. 359-368.
- Jiang H, Aute V, Radermacher R., 2006, CoilDesigner: "A general-purpose simulation and design tool for air-to-refrigerant heat exchangers", *Int. J. of Refrigeration*, Vol. 29: pp. 601-610.
- Judge, J., Radermacher, R., 1997, "A heat exchanger model for mixtures and pure refrigerant cycle simulations", *Int. J. of Refrigeration*, Vol.20, No.4, pp.244-255
- Kays, W. M., London, A. L., 1984, "Compact heat exchangers", 3rd Edition, McGraw-Hill, USA.
- Kim, N. H., Youn, B., Webb, R. L., 1999, "Air-side heat transfer and friction correlations for plain fin-and-tube heat exchangers with staggered tube arrangements", *ASME*, Vol. 121, August.
- Klein, S. A., 2004, EES – "Engineering Equation Solver", F-Chart Software, Madison, WI, USA
- Lemmon, E.W., McLinden, M.O., Klein, S.A., Peskin, A.P., 1998, REFPROP "thermodynamic and transport properties of refrigerants and refrigerant mixtures", NIST Standard Database 23, Version 6.0, Gaithersburg, MD, USA
- Liang, S., Wong, T., Nathan, G., 2001, "Numerical and experimental studies of refrigerant circuitry of evaporator coils", *International Journal of Refrigeration*, Vol. 24: pp. 823-833.
- Schmidt TE, "La Production Calorifique des Surfaces Munies D'ailettes", *Bulletin de L'Institut International du Froid*, Annexe G-5, 1945
- Waltrich, M., 2009, "Projeto e otimização de cassetes de refrigeração para aplicações comerciais leves", Dissertação de Mestrado, Universidade Federal de Santa Catarina, Florianópolis, SC
- Waltrich, P.J., 2008, "Análise e Otimização de Evaporadores de Fluxo Acelerado Aplicados à Refrigeração Doméstica", Dissertação de Mestrado, Universidade Federal de Santa Catarina, Florianópolis, SC
- Wang, C. C., Chang, Y. J., Hsieh, Y. C., Lin, Y. T., 1996, "Sensible heat and friction characteristics of plate fin-and-tube heat exchangers having plane fins", *International Journal of Refrigeration*, Vol. 19: pp. 223-230.
- Wang, C. C., Chi, K. Y., Chang, C. J., 2000, "Heat transfer and friction characteristics of plain fin-and-tube exchangers", part II: Correlation, *Int. J. Heat Mass Transfer*, 43, 2693-2700.
- Weber, G. C., 2007, "Análise experimental do desempenho termo-hidráulico de condensadores do tipo tubo-aletado", Dissertação de Mestrado, Universidade Federal de Santa Catarina, Florianópolis, SC, Brasil.

8. NOMENCLATURE

Roman

A , heat transfer surface, m^2
 A_{face} , heat exchange face area, m^2
 A_{min} , minimum air flow passage, m^2
 C , thermal capacity, W/K
 c_p , specific heat, J/kgK
 d , diameter, m
 f , Darcy friction factor, dimensionless
 F_f , fin pitch, m
 H , height, m
 h , specific enthalpy, J/kg
 L , width, m
 m , mass flow rate, kg/s
 NTU , number of transfer units, dimensionless
 P , depth, m
 p , pressure, Pa
 Q , heat transfer rate, W
 S , spacing, m
 T , temperature, K
 U , overall heat transfer coefficient, W/m^2K
 UA , thermal conductance, W/m^2
 W , power consumption, W

Greek

α , heat transfer coefficient, W/m^2K
 δ , thickness, m
 ε , effectiveness, dimensionless
 η , efficiency, dimensionless
 ρ , density, kg/m^3

Subscripts

a , air
 cv , control volume
 f , fin
 i , inlet
 lo , longitudinal rows
 o , outlet
 r , refrigerant
 t , tube
 tr , transversal rows
 v , fan